Efficient Electrical Spin Splitter Based on Nonrelativistic Collinear Antiferromagnetism

Rafael González-Hernández,[1,2] Libor Šmejkal,[2,3,4] Karel Výborný,[3] Yuta Yahagi,[5] Jairo Sinova,[2,3] Tomáš Jungwirth,[3,6] and Jakub Železný[3]

[1]Grup de Investigación en Física Aplicada, Departamento de Física, Universidad del Norte, Barranquilla 081008, Colombia
[2]Institut für Physik, Johannes Gutenberg Universität Mainz, D-55099 Mainz, Germany
[3]Institute of Physics, Czech Academy of Sciences, Cukrovarnická 10, 162 00 Praha 6, Czech Republic
[4]Faculty of Mathematics and Physics, Charles University in Prague, Ke Karlovu 3, 121 16 Prague 2, Czech Republic
[5]Department of Applied Physics, Tohoku University, Sendai 980-8579, Japan
[6]School of Physics and Astronomy, University of Nottingham, Nottingham NG7 2RD, United Kingdom

(Received 4 August 2020; revised 7 January 2021; accepted 23 February 2021; published 26 March 2021)

Spin-current generation by electrical means is among the core phenomena driving the field of spintronics. Using *ab initio* calculations we show that a room-temperature metallic collinear antiferromagnet RuO_2 allows for highly efficient spin-current generation, arising from anisotropically spin-split bands with conserved up and down spins along the Néel vector axis. The zero net moment antiferromagnet acts as an electrical spin splitter with a 34° propagation angle between spin-up and spin-down currents. The corresponding spin conductivity is a factor of 3 larger than the record value from a survey of 20 000 nonmagnetic spin-Hall materials. We propose a versatile spin-splitter-torque concept circumventing limitations of spin-transfer and spin-orbit torques in present magnetic memory devices.

DOI: 10.1103/PhysRevLett.126.127701

Longitudinal spin-polarized current applied in an out-of-plane direction from a reference to a recording ferromagnetic layer is the basis of commercial, spin-transfer-torque (STT) magnetic random access memories (MRAMs) [1,2]. Here the spin current is due to ferromagnetic exchange splitting, i.e., is odd under time reversal ($\mathcal{T}$). An alternative example is a transverse spin current injected by an applied in-plane charge current from a nonmagnetic relativistic spin-Hall polarizer [3] to the recording magnet in spin-orbit-torque (SOT) devices [4]. Since this $\mathcal{T}$-even spin current does not require a magnetic order, the family of potentially suitable materials is significantly broader. However, this is at the expense of relying on the relativistic spin-orbit coupling, which is typically much weaker than the exchange coupling. Moreover, the same spin nonconserving nature of the spin-orbit coupling that allows for the spin-current generation reduces the spin diffusion length typically to nanoscale, and by this further limits theoretical understanding and practical utility of the relativistic charge-spin conversion phenomena [4].

The family of materials suitable for spin-current generation has been recently expanded by including noncollinear antiferromagnets [5–8]. Remarkably, despite the vanishing net magnetic moment, they allow for the $\mathcal{T}$-odd spin currents in analogy to ferromagnets. However, the noncollinear magnetic order also generates spin-orbit splitting and spin texture in the electronic bands which resemble the relativistic spin-orbit coupling in spin-Hall materials. As a result, spin conservation is broken in noncollinear antiferromagnets even in the nonrelativistic limit [5,6].

In this Letter we predict a distinct spin-current generation mechanism arising from nonrelativistic collinear antiferromagnetism and taking a form of a spin splitter. It requires neither spin-orbit coupling nor noncollinear magnetic order, in stark contrast to the earlier identified mechanisms. As a result, the spin-splitter effect imposes no principle limit on the coherent spin-propagation length. Furthermore, we show in our *ab initio* theory description of a representative collinear antiferromagnet RuO_2, that the resulting spin current is odd under $\mathcal{T}$ and can be pure, i.e., accompanied by a zero parallel charge current.

The spin-current generation in our zero net-moment collinear antiferromagnet is a direct consequence of an anisotropic band spin splitting, schematically illustrated in Figs. 1(a)–1(c). It arises from a collinear exchange coupling between magnetic (Ru) atoms placed in locally anisotropic crystalline environments of the nonmagnetic (O) atoms [9–11]. While the mechanism is applicable in a range of inorganic and organic collinear antiferromagnets [12–14], here we focus on RuO_2 which is a prominent, metallic room-temperature member [9–11,13,15,16] of a textbook family of rutile antiferromagnets [17,18].

Since the spin-current generation effect explored in this Letter is derived directly from the anisotropic spin splitting of the nonrelativistic electronic structure, the calculated conversion ratio between the charge current and the transverse pure spin current is large and only weakly affected by the spin-orbit coupling present in the material. As shown

 © 2021 American Physical Society

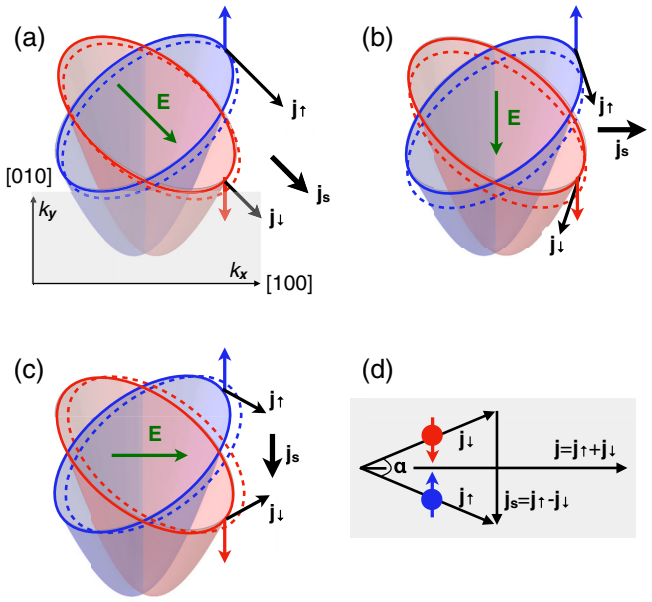

FIG. 1. Schematics of the anisotropic band splitting due to collinear antiferromagnetism and of the spin-splitter effect. (a) For an electric field **E** applied along one of the ⟨110⟩ axes, the spin-up and spin-down charge currents are parallel but of different magnitudes due to the band anisotropies. As a result, the longitudinal charge current is spin polarized. (b),(c) For **E** along one of the ⟨100⟩ axes, the spin-up and spin-down charge currents combine in an unpolarized longitudinal charge current and in a pure transverse spin current. (d) In the absence of relativistic spin-orbit coupling, spin is conserved and the spin-up and spin-down charge currents are split by an angle that is determined by the bands' anisotropy. In RuO_2, the angle $\alpha \approx 34°$.

schematically in Fig. 1(d), the collinear antiferromagnet acts as a direct spin splitter channeling the conserved up- and down-spin electrons at a mutual angle of 34°.

We point out that our spin-splitter effect and the anomalous Hall effect, also recently studied in RuO_2 [9,10], are principally distinct phenomena. While in this Letter we focus on a spin-current response, the Hall effect is a charge-current response. Moreover, the spin-splitter effect is of a nonrelativistic origin which contrasts with the relativistic nature of the anomalous Hall effect. This has both qualitative and quantitative consequences. For example, the anomalous Hall effect is excluded by symmetry when the Néel vector is along the [001] easy axis of RuO_2 [9,10], and when rotating the Néel vector away from the [001] direction the Hall angle reaches only a degree scale [9,10]. In contrast, the nonrelativistic spin-spitter mechanism is present for any Néel vector direction and the large spin-splitter angle is independent of it.

Another principle distinction is that the anomalous Hall effect is primarily used as a detection tool of the magnetic order vector, while the spin-splitter effect belongs to a family of spin-current phenomena which can be used for manipulating the magnetic order. Based on our calculations presented below and referring to the earlier synthesized thin-film materials [10], we propose a concept of a spin-splitter torque (SST) in which an applied in-plane electrical current injects the spin-conserving pure spin-current polarized along the Néel vector in the out-of-plane direction from the RuO_2 film into a recording ferromagnetic layer. As a result of the distinct physical origin, compared to both STT and SOT, our SST mechanism can combine favorable attributes of STT and SOT, while removing their respective key limitations. We will conclude the Letter by illustrative examples of collinear antiferromagnets in which the nonrelativistic spin-splitter effect is absent, and discuss our results in the context of physical phenomena recently associated with a term magnetic spin Hall effect [5,7,8].

In our calculations, we use the density-functional theory (DFT) framework as implemented in the Vienna *ab initio* simulation package (VASP) [19] within the GGA + U approximation [15]. We perform both nonrelativistic calculations and calculations with the relativistic spin-orbit coupling self-consistently included. Electron wave functions are expanded in plane waves up to a cutoff energy of 500 eV and a grid of $12 \times 12 \times 16$ k point is used to sample the irreducible Brillouin zone.

In Figs. 2(a)–2(d) we plot the DFT Fermi surfaces, crystal structure, and DFT charge and magnetization densities in RuO_2. We observe the correspondence between the momentum space and real space representations of the spin-splitter concept. The real space counterpart of the anisotropic band spin splitting are the two intertwined sublattices with their respective anisotropies rotated by 90° [Figs. 2(b) and 2(c)] and one carrying primarily spin-up while the other one spin-down electrons [Fig. 2(d)]. The anisotropic charge densities in Fig. 2(c) may resemble an orbital ordering effect. However, we point out that the structure of RuO_2 differs significantly from, e.g., $KCuF_3$ which represents a canonical material example in studies of orbital ordering [20]. In $KCuF_3$, F-octahedra surrounding the two nonequivalent Cu sites have the same orientation and differ only through small variations in the Cu-F bond lengths (about 3%). In contrast, the O-octahedra corresponding to the different Ru sublattices in RuO_2 are rotated with respect to each other by 90°, as shown in Fig. 2(b). As a result, the Ru-O bond lengths projected on the (001) plane vary by nearly 60%, making the crystalline environment of the Ru sites highly anisotropic.

The spin-splitter angle is governed by the large strength of the sublattice crystalline anisotropies in RuO_2 which give additional parameters like spin-orbit coupling or disorder a minor role. To quantify this, we evaluate the charge to spin-current conversion ratio within the linear response theory using the Kubo formula in the approximation of the constant scattering-rate Γ (corresponding to a constant relaxation-time $\hbar/2\Gamma$), as implemented in the Wannier-Linear-Response code [5,21]. The spin conductivity is described by a tensor σ^a_{bc}, where a corresponds to

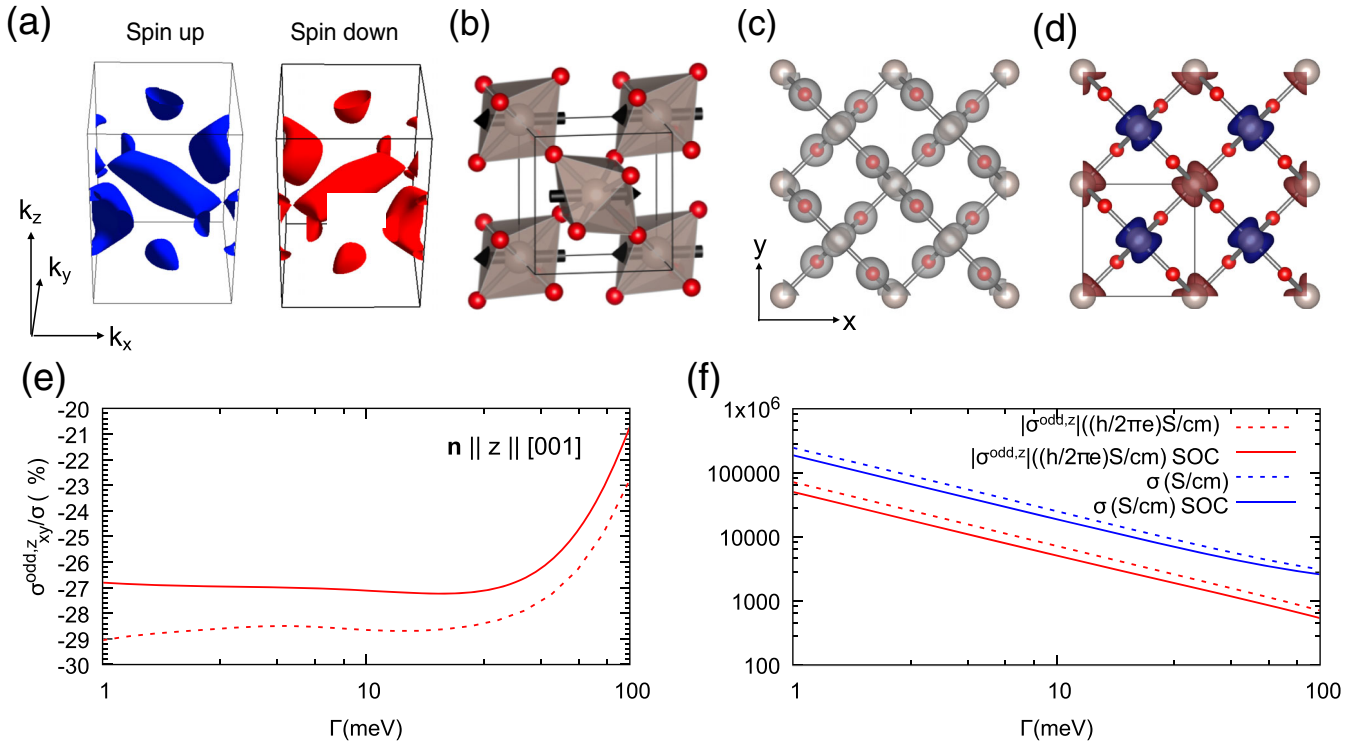

FIG. 2. Electrical spin-splitter effect in RuO_2 from *ab initio* calculations. (a) Spin-up and -down Fermi surfaces. (b) Crystal structure. (c) Anisotropic electronic densities. (d) Anisotropic magnetization densities calculated without spin-orbit coupling [9]. (e) $\mathcal{T}$-odd charge-spin conversion ratio calculated with and without (solid and dashed line) spin-orbit coupling and the Néel vector along the [001] direction. (f) Comparison of the corresponding longitudinal charge conductivity and transverse odd spin conductivity calculated with and without (solid and dashed lines) spin-orbit coupling.

the spin polarization of the spin current, b to the direction of spin-current flow, and c to the direction of the applied electric field. The Kubo formula within the constant Γ approximation can be split into the $\mathcal{T}$-odd contribution [22],

$$\sigma_{bc}^{\mathrm{odd},a} = -\frac{e\hbar}{V\pi}\mathrm{Re}\sum_{\mathbf{k},m,n}\frac{\langle u_n(\mathbf{k})|\hat{J}_b^a|u_m(\mathbf{k})\rangle\langle u_m(\mathbf{k})|\hat{v}_c|u_n(\mathbf{k})\rangle\Gamma^2}{((E_F-E_n(\mathbf{k}))^2+\Gamma^2)(E_F-E_m(\mathbf{k}))^2+\Gamma^2)}, \quad (1)$$

and the $\mathcal{T}$-even contribution given in the $\Gamma \to 0$ limit by

$$\sigma_{bc}^{\mathrm{even},a} = \frac{2e\hbar}{V}\mathrm{Im}\sum_{\mathbf{k},m\neq n}^{\substack{n\,\mathrm{occ.}\\ m\,\mathrm{unocc.}}}\frac{\langle u_n(\mathbf{k})|\hat{J}_b^a|u_m(\mathbf{k})\rangle\langle u_m(\mathbf{k})|\hat{v}_c|u_n(\mathbf{k})\rangle}{(E_n(\mathbf{k})-E_m(\mathbf{k}))^2}. \quad (2)$$

Here $u_n(\mathbf{k})$ are the Bloch functions of a band n, $\mathbf{k}$ is the Bloch wave vector, $\varepsilon_n(\mathbf{k})$ is the band energy, E_F is the Fermi energy, $\hat{v}$ is the velocity operator, e is the elementary charge ($e > 0$), and the spin-current operator $\hat{J}_b^a = \frac{1}{2}\{\hat{s}_a, \hat{v}_b\}$. In order to evaluate the Kubo formula, we construct an effective tight-binding Hamiltonian in the maximally localized Wannier basis [23] as a postprocessing step of the DFT calculations. For the integration, we use a dense 320^3 $\mathbf{k}$-mesh.

For small Γ, the Kubo formula (1) for $\sigma_{bc}^{\mathrm{odd},a}$, which describes our spin-splitter effect, scales as $1/\Gamma$ and is equivalent to the semiclassical Boltzmann equation with constant scattering rate. In RuO_2, $\Gamma = 6.6$ meV corresponds to an average experimental value of the room-temperature charge conductivity $\sigma = 2.8 \times 10^4\ \Omega^{-1}\,\mathrm{cm}^{-1}$ [24]. This value of Γ is safely below the upper limit ($\sim$100 meV) of the $1/\Gamma$ scaling of $\sigma_{bc}^{\mathrm{odd},a}$ and σ ($= \sigma_{xx}$), as shown in Fig. 2(e). The $\mathcal{T}$-odd charge-spin conversion ratio $\sigma_{bc}^{\mathrm{odd},a}/\sigma$ is then only weakly dependent on disorder scattering, as anticipated above and confirmed numerically in Fig. 2(d).

While $\sigma_{bc}^{\mathrm{odd},a}$ diverges for $\Gamma \to 0$, $\sigma_{bc}^{\mathrm{even},a}$ is finite in the clean limit and described by the intrinsic Kubo formula (2). It implies that the corresponding conversion ratio $\sigma_{bc}^{\mathrm{even},a}/\sigma \to 0$ for $\Gamma \to 0$. Since the intrinsic contribution often dominates in the favorable, strongly spin-orbit coupled materials [3], this is a significant limiting factor of the $\mathcal{T}$-even charge-spin conversion in metals. The $\mathcal{T}$-odd part circumvents this limitation in metallic systems and it also circumvents the spin-loss inherent to the $\mathcal{T}$-even spin

conductivity [5,6]. This is highlighted in Fig. 2(e), where we show that the effect of the relativistic spin-orbit coupling on the $\mathcal{T}$-odd charge-spin conversion ratio is weak, despite the presence of significant spin-orbit coupling in the material due to the heavy element Ru [cf. Fig. 2(e)]. Figure 2(f) thus confirms the efficiency and the nonrelativistic spin-splitter nature of the phenomenon in RuO_2. The calculated charge-spin conversion ratio $\sigma_{bc}^{\mathrm{odd},a}/\sigma \approx 28\%$ which corresponds to the angle between the spin-up and spin-down transport channels of 34° [Fig. 1(e)]. We point out that our spin-splitter conversion ratio is significantly larger than the experimentally reported charge-spin conversion ratios (angles) in the most extensively explored spin-Hall metal Pt, and comparable to the record metallic spin-Hall conversion material β-W [3].

The $\sigma_{bc}^{\mathrm{odd},a}$ calculations shown in Figs. 2(d) and 2(e) are for the $b = x$ ([100]) and $c = y$ ([010]) crystal directions in tetragonal RuO_2. Without relativistic spin-orbit coupling, $\sigma_{xy}^{\mathrm{odd},a} = \sigma_{yx}^{\mathrm{odd},a}$ [cf. Figs. 1(b) and 1(c)] are the only nonzero $\mathcal{T}$-odd spin-conductivity components in the material, which can be formally verified using the symmetry group analysis [6,25]. The spin polarization of the nonrelativistic spin current is along the spin quantization axis of the electronic structure, i.e., is aligned with the axis of the Néel vector $\mathbf{n}$. Calculations in Figs. 2(d) and 2(e) were done for $\mathbf{n} \| [001]$ and we, therefore, plot the $a = z$ ([001]) component of $\sigma_{xy}^{\mathrm{odd},a}$. Note that when spin-orbit coupling is included, more components of $\sigma_{bc}^{\mathrm{odd},a}$ are allowed by symmetry, as summarized in the Supplemental Material [26].

In Fig. 3(a) we show that the spin-orbit coupling has a weak effect on the charge-spin conversion ratio also when the Néel vector is in the x-y plane of RuO_2. The cosine dependence of the plotted $\sigma_{xy}^{\mathrm{odd},x}$ as a function of the in-plane Néel vector angle measured from the x axis again reflects that the spin polarization of the leading nonrelativistic contribution to the spin current is aligned with $\mathbf{n}$. In Fig. 3(b) we show for comparison the $\mathcal{T}$-even charge-spin conversion ratio for the spin-Hall component $\sigma_{xy}^{\mathrm{even},z} = -\sigma_{yx}^{\mathrm{even},z}$ in RuO_2. For the experimental value of $\Gamma = 6.6$ meV, the nonrelativistic $\mathcal{T}$-odd spin splitter outperforms by 2 orders of magnitude the $\mathcal{T}$-even spin-Hall effect, which is of relativistic origin in RuO_2 as in nonmagnets [3] (see Supplemental Material [26]). We also point out here that our calculated nonrelativistic $\mathcal{T}$-odd spin conductivity in RuO_2 is a factor of 3 larger than the record value of the relativistic $\mathcal{T}$-even spin-Hall conductivity from a survey of 20 000 nonmagnetic materials [34].

Regarding the robustness of the spin-splitter effect in RuO_2 we recall that the magnetocrystalline anisotropy is dominated by a strong easy-axis energy term of ~1 meV per unit cell along the tetragonal c axis ([001] direction) [9,10]. RuO_2 thus belongs to a family of exceptionally magnetically hard antiferromagnets [35], which justifies our DFT calculations of the spin-splitter effect with a static

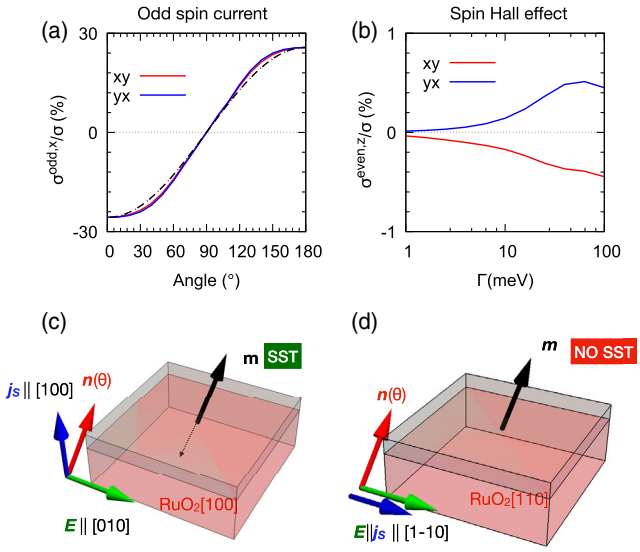

FIG. 3. Spin-splitter-torque concept. (a) $\mathcal{T}$-odd spin-splitter charge-spin conversion ratio as a function of the in-plane Néel vector angle highlighting that the polarization of the spin current follows the Néel vector. (b) $\mathcal{T}$-even spin-Hall charge-spin conversion ratio as a function of the scattering rate. (c),(d) Schematics of antiferromagnetic (red)–ferromagnetic (gray) bilayer with two different orientations of the RuO_2 crystal. Configuration (c) gives a spin current in the antiferromagnet propagating in the out-of-plane direction, which can generate a spin-splitter torque on the magnetization of the ferromagnet. Configuration (d) gives an in-plane spin current and, therefore, generates no spin-splitter torque.

Néel vector and neglected magnetic excitations. However, when approaching the transition temperature, the spin current due to the spin-splitter effect will inevitably get suppressed. In analogy to spin-polarized currents in ferromagnets, this is because of the reduced (sublattice) magnetization and corresponding suppression of the band spin splitting, as well as due to electron-magnon scattering.

We now discuss the utility of the spin-splitter concept in spin-torque structures. We recall that STT based on the $\mathcal{T}$-odd spin-polarized current mechanism employed in commercial MRAMs suffers from some limitations given by the two-point out-of-plane geometry of both the electrical STT writing and the electrical readout by tunneling magnetoresistance. One particular challenge in STT-MRAMs is to balance a sufficiently large separation between writing and readout currents with strong enough readout signals and with writing currents kept safely below the breakdown threshold of the tunnel barrier [1,2]. Research and development of SOT MRAMs based on the $\mathcal{T}$-even spin-Hall currents is fueled in large part by the possibility to employ a three-point geometry with an in-plane Ohmic path for the writing electrical current. However, they rely on the spin-orbit coupling which is spin nonconserving and more subtle than the ferromagnetic exchange. Both these features can limit the SOT efficiency.

Our SST, illustrated in Fig. 3(c), shares the versatility of STT offered by the control of the $\mathcal{T}$-odd spin current by the magnetic order. Simultaneously, it does not inherit the problems of STT associated with the applied out-of-plane electrical writing current. Instead, SST shares the in-plane electrical writing geometry of SOT while circumventing the spin-loss limitations of the $\mathcal{T}$-even spin currents.

In Fig. 3(c) we consider a RuO_2-ferromagnet bilayer grown along the [100] crystal axis, as reported in Ref. [10]. This is the optimal geometry for SST. Here the electric field applied along the in-plane [010] axis generates the pure nonrelativistic spin current along the out-of-plane [100] direction with the polarization of the spin current determined by the Néel vector [cf. Fig. 1(b)]. In stoichiometric RuO_2, the Néel vector easy axis is along the [001] direction [9,10,15], which implies efficient SST for switching of an in-plane magnetized ferromagnet interfaced with RuO_2.

The easy axis in RuO_2 can be rotated into the (001)-plane by off stoichiometry or alloying (with, e.g., Ir) [9] in which case SST is optimized for switching an out-of-plane magnetized ferromagnet. On the other hand, a RuO_2 film grown along the [110] axis [10] only allows for generating a longitudinal spin-polarized current propagating along the applied in-plane ($\|[1\bar{1}0]$) electric field. This is seen in the model anisotropic spin-split bands in Fig. 1(a) and can be formally obtained from the calculated $\sigma_{xy}^{\mathrm{odd},a} = \sigma_{yx}^{\mathrm{odd},a}$ components by rotating the Cartesian coordinates by 45°. The geometry precludes the SST switching of the interfaced ferromagnet [Fig. 3(d)], a feature that can be used to test the SST phenomenology in experiment. Note that a longitudinal spin-polarized current propagating along an applied out-of-plane ($\|[110]$) electric field could be used for the STT switching of the adjacent ferromagnet. We also recall here that the $\mathcal{T}$-odd spin current is predicted to be 2 orders of magnitude larger than the $\mathcal{T}$-even spin current [cf. Figs. 3(a) and 3(b)]. Experimentally disentangling the SST in RuO_2-ferromagnet bilayers grown along the [100] crystal axis from the SOT contribution should, therefore, be readily feasible.

We conclude our discussion with a few remarks on the spin-splitter effect in broader materials and charge-spin conversion contexts. The spin-splitter effect in which an electrical current generates a pure conserving spin current requires a collinear antiferromagnet. However, not all collinear antiferromagnets have the effect allowed by symmetry. The spin conductivity is invariant under spatial translation (t) or inversion ($\mathcal{P}$), and the $\mathcal{T}$-odd spin conductivity requires $\mathcal{T}$-symmetry breaking. This implies that it is excluded in systems with combined $t\mathcal{T}$ or $\mathcal{PT}$ symmetries. FeRh or CuMnAs are examples of materials used in spintronics research of metallic collinear antiferromagnets [36] falling into this high-symmetry category, and which therefore do not show this effect. MnTe, another prominent material in antiferromagnetic spintronics research [37], is a different case. This collinear semiconducting antiferromagnet has both the $t\mathcal{T}$ and $\mathcal{PT}$ symmetries broken and the $\mathcal{T}$-odd spin conductivity is allowed in this material, as in all crystals breaking $t\mathcal{T}$ and $\mathcal{PT}$. However, it requires spin-orbit coupling while the nonrelativistic spin-splitter effect is absent in MnTe. (For a detailed comparison between MnTe and RuO_2 see the Supplemental Material [26]).

Finally, we point out that both $\mathcal{T}$-odd and $\mathcal{T}$-even spin conductivity tensors can have symmetric and antisymmetric components (i.e., also longitudinal and transverse components) for a general crystal symmetry. This is in contrast to the charge conductivity tensor whose $\mathcal{T}$-even part is purely symmetric and $\mathcal{T}$-odd part purely antisymmetric. As a result, there is some ambiguity in the terminology of the charge-spin conversion phenomena [5–8,27,38]. Traditionally, when focusing on isotropic models, the term spin Hall effect has been more narrowly reserved to the antisymmetric part of the $\mathcal{T}$-even spin conductivity [3]. However, in lower symmetry crystals, the symmetric $\mathcal{T}$-even spin conductivity can be also allowed. The term spin Hall effect has been then used in a broader sense to capture the full $\mathcal{T}$-even spin conductivity tensor, including its antisymmetric and symmetric components [6,8]. Similar ambiguity exists with the recently introduced term magnetic spin Hall effect in the context of studies of the $\mathcal{T}$-odd spin conductivity in noncollinear antiferromagnets [5,7,8]. Our nonrelativistic spin-splitter effect in RuO_2 is described by the symmetric $\mathcal{T}$-odd spin conductivity and can, therefore, be considered to fall within the family of magnetic spin Hall effects in the broader sense of the term.

We acknowledge funding from the Czech Science Foundation Grant No. 19-18623Y, the Ministry of Education of the Czech Republic Grants No. LM2018096, No. LM2018110, No. LM2018140, and No. LNSM-LNSpin, and the EU FET Open RIA Grant No. 766566, Deutsche Forschungsgemeinschaft Grant No. TRR 173 268565370 (project A03), support from the Max Planck Partner Group programme, the computing time granted on the supercomputer Mogon at Johannes Gutenberg University Mainz (hpc.uni-mainz.de) and the support of the Alexander Von Humboldt Foundation.

[1] D. C. Ralph and M. D. Stiles, J. Magn. Magn. Mater. **320**, 1190 (2008).
[2] A. Brataas, A. D. Kent, and H. Ohno, Nat. Mater. **11**, 372 (2012).
[3] J. Sinova, S. O. Valenzuela, J. Wunderlich, C. H. Back, and T. Jungwirth, Rev. Mod. Phys. **87**, 1213 (2015).
[4] A. Manchon, J. Železný, I. M. Miron, T. Jungwirth, J. Sinova, A. Thiaville, K. Garello, and P. Gambardella, Rev. Mod. Phys. **91**, 035004 (2019).
[5] J. Železný, Y. Zhang, C. Felser, and B. Yan, Phys. Rev. Lett. **119**, 187204 (2017).

[6] Y. Zhang, J. Železný, Y. Sun, J. van den Brink, and B. Yan, New J. Phys. **20**, 073028 (2018).
[7] M. Kimata, H. Chen, K. Kondou, S. Sugimoto, P. K. Muduli, M. Ikhlas, Y. Omori, T. Tomita, A. H. MacDonald, S. Nakatsuji, and Y. Otani, Nature (London) **565**, 627 (2019).
[8] A. Mook, R. R. Neumann, A. Johansson, J. Henk, and I. Mertig, Phys. Rev. Research **2**, 023065 (2020).
[9] L. Šmejkal, R. González-Hernández, T. Jungwirth, and J. Sinova, Sci. Adv. **6**, eaaz8809 (2020).
[10] Z. Feng, X. Zhou, L. Šmejkal, L. Wu, Z. Zhu, H. Guo, R. González-Hernández, X. Wang, H. Yan, P. Qin, X. Zhang, H. Wu, H. Chen, C. Jiang, M. Coey, J. Sinova, T. Jungwirth, and Z. Liu, arXiv:2002.08712.
[11] K.-H. Ahn, A. Hariki, K.-W. Lee, and J. Kuneš, Phys. Rev. B **99**, 184432 (2019).
[12] M. Naka, S. Hayami, H. Kusunose, Y. Yanagi, Y. Motome, and H. Seo, Nat. Commun. **10**, 4305 (2019).
[13] S. Hayami, Y. Yanagi, and H. Kusunose, J. Phys. Soc. Jpn. **88**, 123702 (2019).
[14] L.-D. Yuan, Z. Wang, J.-W. Luo, E. I. Rashba, and A. Zunger, arXiv:1912.12689.
[15] T. Berlijn, P. C. Snijders, O. Delaire, H. D. Zhou, T. A. Maier, H. B. Cao, S. X. Chi, M. Matsuda, Y. Wang, M. R. Koehler, P. R. Kent, and H. H. Weitering, Phys. Rev. Lett. **118**, 077201 (2017).
[16] Z. H. Zhu, J. Strempfer, R. R. Rao, C. A. Occhialini, J. Pelliciari, Y. Choi, T. Kawaguchi, H. You, J. F. Mitchell, Y. Shao-Horn, and R. Comin, Phys. Rev. Lett. **122**, 017202 (2019).
[17] M. Tinkham, *Physics Bulletin* (Dover Publications, New York, 1964).
[18] C. A. Corrêa and K. Výborný, Phys. Rev. B **97**, 235111 (2018).
[19] G. Kresse and J. Furthmüller, Phys. Rev. B **54**, 11169 (1996).
[20] E. Pavarini, E. Koch, and A. I. Lichtenstein, Phys. Rev. Lett. **101**, 266405 (2008).
[21] J. Zelezny, https://bitbucket.org/zeleznyj/wannier-linear-response/wiki/Home.
[22] F. Freimuth, S. Blügel, and Y. Mokrousov, Phys. Rev. B **90**, 174423 (2014).
[23] A. A. Mostofi, Comput. Phys. Commun. **178**, 685 (2008).
[24] W. D. Ryden, A. W. Lawson, and C. C. Sartain, Phys. Rev. B **1**, 1494 (1970).
[25] J. Železný, https://bitbucket.org/zeleznyj/linear-response-symmetry.
[26] See Supplemental Material at http://link.aps.org/supplemental/10.1103/PhysRevLett.126.127701 for the analysis of the spin conductivity tensors in RuO_2 and MnTe, general symmetry analysis of $\mathcal{T}$-odd spin currents, and RuO_2 and MnTe band structures, which includes Refs. [7,9,25,27–33].
[27] M. Seemann, D. Ködderitzsch, S. Wimmer, and H. Ebert, Phys. Rev. B **92**, 155138 (2015).
[28] J. Železný, H. Gao, A. Manchon, F. Freimuth, Y. Mokrousov, J. Zemen, J. Mašek, J. Sinova, and T. Jungwirth, Phys. Rev. B **95**, 014403 (2017).
[29] S. Zhang and O. Tchernyshyov, Phys. Rev. B **98**, 104411 (2018).
[30] J. Železný, Y. Zhang, C. Felser, and B. Yan, Phys. Rev. Lett. **119**, 187204 (2017).
[31] S. Shtrikman and H. Thomas, Solid State Commun. **3**, 147 (1965).
[32] *International Tables for Crystallography*, edited by T. Hahn, 1st ed. (International Union of Crystallography, Chester, 2006), Vol. A.
[33] G. Yin, J.-X. Yu, Y. Liu, R. K. Lake, J. Zang, and K. L. Wang, Phys. Rev. Lett. **122**, 106602 (2019).
[34] Y. Zhang, Q. Xu, K. Koepernik, J. Železný, T. Jungwirth, C. Felser, J. van den Brink, and Y. Sun, arXiv:1909.09605.
[35] L. Szunyogh, B. Lazarovits, L. Udvardi, J. Jackson, and U. Nowak, Phys. Rev. B **79**, 020403(R) (2009).
[36] T. Jungwirth, X. Marti, P. Wadley, and J. Wunderlich, Nat. Nanotechnol. **11**, 231 (2016).
[37] D. Kriegner, K. Výborný, K. Olejník, H. Reichlová, V. Novák, X. Marti, J. Gazquez, V. Saidl, P. Němec, V. V. Volobuev, G. Springholz, V. Holý, and T. Jungwirth, Nat. Commun. **7**, 11623 (2016).
[38] S. Wimmer, M. Seemann, K. Chadova, D. Ködderitzsch, and H. Ebert, Phys. Rev. B **92**, 041101(R) (2015).